

Crystal Chemistry of Layered Manganites $\text{Ln}_{1.4}\text{Sr}_{1.6}\text{Mn}_2\text{O}_7$ (Ln = La, Pr, Nd, Sm, Eu, and Gd)

Eun-Ok Chi, Young-Uk Kwon,* and Nam Hwi Hur[†]

Department of Chemistry, Sungkyunkwan University, Suwon 440-746, Korea

[†]Korea Research Institute of Science and Standards, Taejeon 306-600, Korea

Received June 17, 1999

The powder X-ray diffraction patterns of a series of layered manganite compounds, $\text{Ln}_{1.4}\text{Sr}_{1.6}\text{Mn}_2\text{O}_7$ (Ln = La, Pr, Nd, Sm, Eu, Gd), were refined with the Rietveld method. The Ln occupancy in the rock salt site increases on moving from La through Gd. The variations of the lattice parameters and the bond distances correlate and can be accounted for with the distribution of Ln and Sr in the perovskite and rock salt sites. The structural analysis implies that the physical properties of these compounds have to vary monotonically from La through Sm and then more or less the same from Sm through Gd, which is not the case. Therefore, in order to understand the various physical properties of these compounds depending on Ln another factors such as the magnetic properties of Ln need to be considered.

Introduction

Recent interests in the colossal magnetoresistant (CMR) $n = 2$ Ruddlesden-Popper (RP) type layered manganites of the general formula $\text{Ln}_{2-2x}\text{Sr}_{1+2x}\text{Mn}_2\text{O}_7$ stimulated much research effort to understand the nature of the physical properties of these compounds.^{1,4} Especially, compounds with Ln = La have been extensively studied with various hole doping levels (x).^{5,6} The hole doping level is found to strongly influence the physical properties of these compounds. On the other hand, there has been relatively less attention on the possibility of Ln variation. There are some papers on the Ln = Nd compounds with different hole doping levels.⁷⁻¹⁰ Indeed, these compounds show much different magnetic and transport properties from those of La-containing ones. However, the compounds with other Ln ions of this system have not been studied. Therefore, besides the influence of the hole doping level, many other factors that can influence the physical properties of these compounds remain unexplored.

We have previously reported our results of a systematic study on the $\text{Ln}_{1.4}\text{Sr}_{1.6}\text{Mn}_2\text{O}_7$ (Ln = La, Pr, Nd, Sm, Eu, Gd) system for the synthesis and magnetic and transport properties.^{11,12} These compounds show remarkable dependency of the physical properties on Ln. Because the variation of Ln can influence the crystal structures which, in turn, can influence the physical properties of these compounds, we have analyzed the crystal structures of these compounds to understand the underlying physics of these systems.

In this paper, through Rietveld analyses of the powder X-ray diffraction data of these compounds, we show that the variation of Ln is reflected in many aspects of the crystal chemistry of this system. The implication of the Ln substitution and thus the crystal chemistry on the physical properties is discussed along with the influence of the other factors such as the magnetic properties of Ln ions.

Experimental Section

Polycrystalline samples of $\text{Ln}_{1.4}\text{Sr}_{1.6}\text{Mn}_2\text{O}_7$ (Ln = La, Pr, Nd, Sm, Eu, Gd) were prepared by solid state reaction.^{11,12} Stoichiometric mixtures of oxides and carbonates of corresponding metals were calcined at 1000 °C and sintered at 1400-1500 °C in air with intermittent grinding and pelletizing. La_2O_3 were heat treated at 700 °C prior to use.

Powder X-ray diffraction (PXRD) patterns for the Rietveld structure refinements were obtained using a Rigaku RAD X-ray powder diffractometer using Cu-K α radiation in Bragg-Brentano geometry. The step scan conditions are angular range of $5^\circ \leq 2\theta \leq 100^\circ$ with an interval size of 0.02° and a counting time of 10 seconds for each step. For the Rietveld profile analyses, RIETAN program was used.^{13,14} In the refinements, the background was fitted with a 12-term Legendre polynomial, and Pseudo-Voigt profile-shape function and March-Dollase preferred-orientation function were used.

Results and Discussion

In their paper on a series of c $\text{LnSr}_2\text{Mn}_2\text{O}_7$ compounds, Battle *et al.* argued that their samples with early Ln (Ln = La-Gd) in fact contained two $n = 2$ RP phases with slightly different lattice parameters. They showed that the X-ray diffraction peak shapes, such as for (0 0 10) reflection, could be fit with the two phase model much better than a single phase model.^{7,9} We have attempted the same type of analysis on our diffraction data to conclude that our sample did not have such two phase mixing problem. The peak shape of the (0 0 10) diffraction of our Ln = Gd compound shown in Figure 2 as an example clearly shows that there is no second $n = 2$ RP phase. However, the Rietveld refinements of our samples show that there are perovskite type impurity phases by 2-3%.

The Rietveld refinement results of our PXRD data are

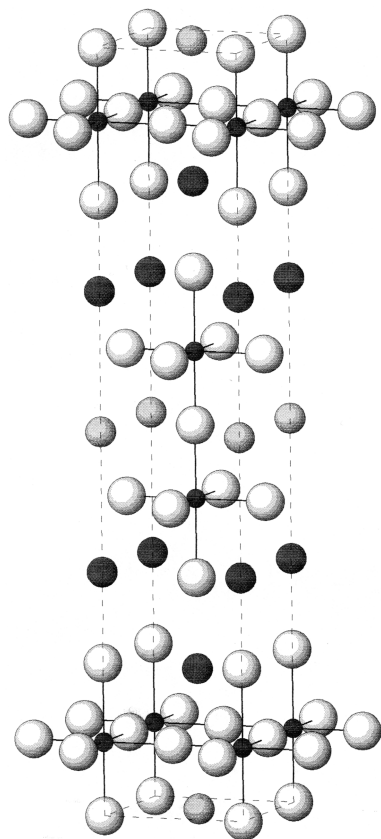


Figure 1. Structure and labeling scheme of the $n = 2$ Ruddlesden-Popper structure.

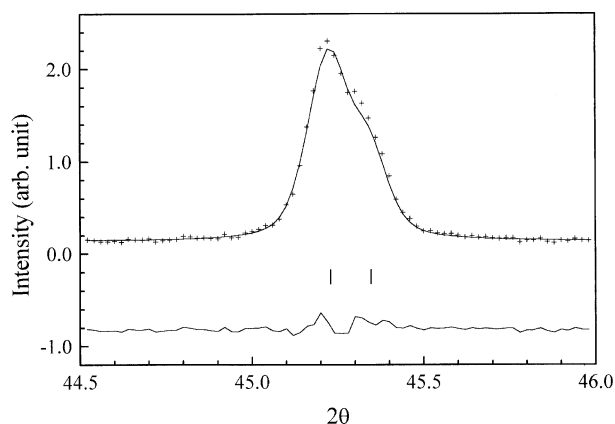


Figure 2. Peak shape of the (0 0 10) reflection of $\text{Gd}_{1.4}\text{Sr}_{1.6}\text{Mn}_2\text{O}_7$. The two tick marks are from the $K\alpha_1$ and $K\alpha_2$ radiations of Cu target.

summarized in Table 1. The occupation factors of Ln and Sr on the perovskite (P) and the rock salt (R) sites were refined with constraints of full occupations on both of the sites and the total Ln/Sr ratio the same as the nominal value of 1.4/1.6. The tetragonal lattice parameters vary with the radius of the Ln atom. Figure 3 shows that the unit cell volume decreases monotonically with the average ionic radius of Ln and Sr, $\langle r \rangle_{\text{ave}}$. Shannons ionic radii for CN = 9 [15] were used for these plots and those in the following discussion. However, as can be seen in Figure 3b, the variations of the a- and c-

Table 1. Rietveld refinement results of the powder X-ray diffraction data of $\text{Ln}_{1.4}\text{Sr}_{1.6}\text{Mn}_2\text{O}_7$ (Ln = La, Pr, Nd, Sm, Eu, Gd) (Space group; $I4/mmm$)

Ln	La	Pr	Nd	Sm	Eu	Gd
Ln/Sr(2)						
Z^a	0.3170(3)	0.3176(3)	0.3170(3)	0.3168(2)	0.3166(2)	0.3164(3)
B_{iso}	0.6(2)	1.5(3)	0.9(2)	0.4(2)	0.3(1)	0.5(2)
Mn						
Z^a	0.0975(6)	0.0973(6)	0.0972(8)	0.0970(5)	0.0975(6)	0.0980(6)
B_{iso}	0.3(2)	0.08(0.2)	0.9(2)	0.1(2)	0.003(0.2)	0.02(0.2)
O(2)						
Z^a	0.197(2)	0.199(2)	0.201(3)	0.200(2)	0.200(3)	0.202(2)
B_{iso}	1.6(5)	1.2(1.1)	0.9(2)	2.4(5)	4.9(1.6)	2.9(1.3)
O(3)						
Z^a	0.095(2)	0.096(2)	0.098(2)	0.100(2)	0.101(4)	0.101(2)
B_{iso}	1.6(6)	1.6(7)	0.9(2)	2.4(5)	1.0(7)	1.1(7)
a (Å)	3.8686(6)	3.8492(3)	3.8495(6)	3.8217(2)	3.8161(6)	3.8164(9)
c (Å)	20.238(4)	20.222(2)	20.214(4)	20.2137(9)	20.131(4)	20.059(6)
R_{wp}	12.36	13.87	14.50	12.51	10.55	10.28
R_{p}	9.53	10.70	11.47	9.51	8.18	7.18
S	1.4	1.4	1.4	2.1	1.8	1.9

^aAtomic positions: Ln/Sr(1) (2b); 0, 0, 0.5, Ln/Sr(2) (4e); 0, 0, z, Mn (4e); 0, 0, z, O(1) (2a); 0, 0, 0, O(2) (4e); 0, 0, z, O(3) (8g); 0, 0.5, z.

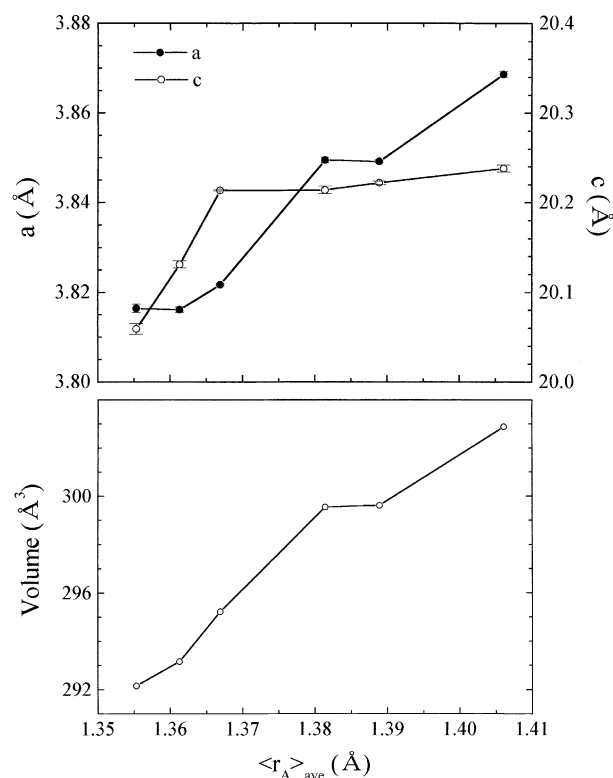


Figure 3. Cell parameters and volumes of $\text{Ln}_{1.4}\text{Sr}_{1.6}\text{Mn}_2\text{O}_7$ (Ln = La, Pr, Nd, Sm, Eu, Gd) as a function of the average ionic radius of Ln and Sr from the Rietveld refinements on the powder X-ray diffraction patterns.

parameters do not seem to reflect the $\langle r \rangle_{\text{ave}}$ changes directly. In the range of Ln = La-Sm, the a-parameter decreases while the c-parameter is held nearly constant as $\langle r \rangle_{\text{ave}}$ decreases. On passing Sm, the trends are reversed and the c-parameter

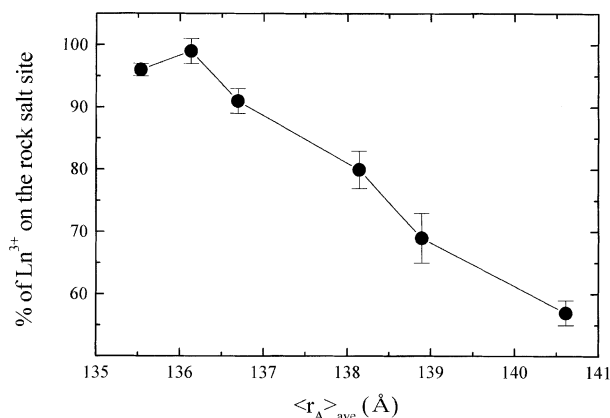


Figure 4. Variation of the occupancy factor of Ln in the rock salt site as a function of the average ionic radius of Ln and Sr from the Rietveld refinements of the powder X-ray diffraction patterns.

shows an abrupt decrease while the *a*-parameter is held almost constant.

The refined relative Ln/Sr occupancies on the two (P and R) sites also show interesting variations with $\langle r \rangle_{\text{ave}}$. The Ln = La compound has 57(2)% of total La in the R-site, smaller than 66.7% in a random model. However, as $\langle r \rangle_{\text{ave}}$ decreases the proportion of Ln (Ln in the R-site/total Ln (= 1.4)) in this site increases monotonically to a saturation of 99(2)% and 96(1)% for Ln = Eu and Gd, respectively. (Figure 4) These data imply that the preference of the Ln atoms for the R-site increases with decreasing $\langle r \rangle_{\text{ave}}$ so that almost all of Ln goes in the R-site for Ln smaller than Sm. There are many factors that govern the distribution of Ln/Sr between the two sites. The R-site is 9-coordinate while the P-site is 12-coordinate. The size of the P-site appears to be restricted by the Mn-O framework in the perovskite-like 3D structure while the R-site appears to have a freedom to adjust with the size of Ln/Sr by changing the interlayer distance. The Madelung type site potential calculations for the two sites resulted in a slightly higher potential on the R-site than on the P-site implying that the R-site has a preference for Ln over Sr. Most of all, we believe that the size matching between the Ln/Sr ions and the hole of the perovskite type Mn-O framework is the governing factor that determines the Ln/Sr distribution. In order to quantify this idea we have calculated the tolerance factor (t_k) based on the refined occupancy and the random distribution model. Unfortunately, some of the ionic radii of Ln^{3+} ions for coordination number 12 are not available to be used for these calculations. Therefore, we have fitted the ionic radii for various coordination numbers of a Ln ion to an exponential function $r(\text{CN} = m) = r(\text{CN} = 1) + a \cdot \log(m)$ where $r(\text{CN} = 1)$ and a are refinable parameters to get a good relationship, and extrapolated these curves to CN = 12 to get the values in Table 2. The relationship between the bond distance(*d*) with the bond order(*n*), $d(n) = d(1) - 0.300 \log n$, is well established.¹⁶ The equation used is just a different expression of this taking that the bond order is inversely proportional to the coordination number into consideration. Also, we have confirmed that the available data

Table 2. Tolerance factors for the perovskite site, and Jahn-Teller(D) and distortion(σ) parameters of the MnO_6 octahedra of $\text{Ln}_{1.4}\text{Sr}_{1.6}\text{Mn}_2\text{O}_7$ (Ln = La, Pr, Nd, Sm, Eu, Gd)

Ln	La	Pr	Nd	Sm	Eu	Gd
$r_{\text{Ln}}(\text{CN}=12)$ (pm)	150	145.43 ^a	141	138	138.05 ^a	136.38 ^a
refined $\langle r_A \rangle_{\text{P}}$	153.18	152.53	153.24	155.48	157.72	156.79
occupancy (pm) t_k	0.982	0.979	0.982	0.990	0.998	0.995
random $\langle r_A \rangle_{\text{P}}$	154.24	152.13	150.01	148.60	148.69	147.91
model (pm) t_k	0.986	0.978	0.971	0.966	0.966	0.964
D ^b	0.972	0.955	0.946	0.945	0.948	0.942
σ^b	0.0278	0.0498	0.0638	0.0648	0.0588	0.0655

^aCalculated by extrapolation of the literature data. ^bFor definitions, see text.

for $r(\text{CN} = 12)$ data of some Ln^{3+} ions do obey this relationship very well as shown in Figure 5. In Table 2, we show the calculated tolerance factors using so obtained and reported $r(\text{CN} = 12)$ data. Although t_k increases slightly with decreasing $\langle r \rangle_{\text{ave}}$, these values are remarkably constant and are close to the ideal value of unity, indicating that the Ln/Sr distribution indeed is related with the size matching between the Ln/Sr ions and the hole size of the P-site. The slight increase of t_k can be related with the Mn-O(2)-Mn bond angle variation (below). Therefore, the increase of Ln population with the decrease of $\langle r \rangle_{\text{ave}}$ is mainly because that more of larger Sr is required for the P-site to meet the hole size of the Mn-O framework. The Mn-O framework thus can maintain its almost ideal structure as in the ideal cubic perovskite. This conclusion gains further support when t_k values for the random model are compared which give large deviations from the ideal value of unity especially for the compounds of smaller Ln. (Table 2) The smaller La occupancy at the R-site than in the random distribution model for the Ln = La compound, despite that the R-site has a preference for La over Sr, can thus be understood by this size matching mechanism.

The variations of the bond distances with $\langle r \rangle_{\text{ave}}$ appear to

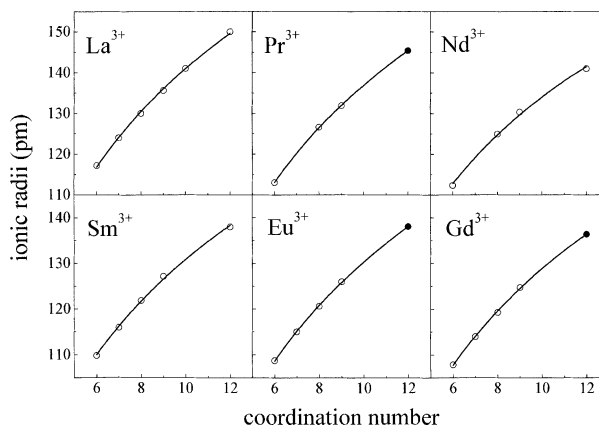


Figure 5. Ionic radii of Ln^{3+} ions as a function of the coordination number. The open circles are from the literature and the filled circles are the extrapolated values to the coordination number 12 of the curves obtained from fitting the data to a $r(\text{CN} = n) = r(\text{CN} = 1) + a \cdot \log(n)$ function.

reflect the change of the Ln/Sr distribution. As above calculations of t_k show, the size of the R-site decreases on moving from La to Sm because of the increasing occupancy of Ln in this site, but that of the P-site is almost unchanged. In order to accommodate the size reduction of the R-site, the interfacial plane between the perovskite and the rock salt layers, the ab-plane, also has to decrease resulting in the decrease of the a-parameter which is reflected by the decrease of the Mn-O(3) bond distance. The slight decrease of Mn-O(1) along the c-direction in the perovskite layer may be explained with the isotropic compression of the $\langle r \rangle_P$. The compression of these five Mn-O bonds requires the Mn-O(2) bond to increase by a large amount. On the other hand, the increased Ln population in the R-site reduces the average Ln/Sr-O(2) distance as $\langle r \rangle_{ave}$ decreases. The nearly compensating and opposite changes of the Mn-O(2) and Ln/Sr-O(2) distances result in nearly constant c-parameter for Ln = La-Sm compounds. As the Ln occupancy becomes saturated in the R-site for Gd and Eu compounds, above mechanism is no longer effective. Therefore, the Mn-O(2) distance stops showing significant increase from Sm on, while the Ln/Sr-O(2) distances continue to decrease due to the reduced $\langle r \rangle_{ave}$ to result in a decrease of the c-parameter for Eu and Gd compounds.

The variation of the Mn-O(3)-Mn bond angle within the ab-plane provides an insight on another aspect of the relative size of the $\langle r \rangle$ of Ln/Sr in the P-site and the hole size of the perovskite. The other Mn-O(1)-Mn bond angle is 180° because of the symmetry requirement. The Mn-O(3)-Mn bond angle here is defined as the angle view from the rock salt layer to the perovskite layer. Therefore, bond angles larger than 180° means that the O(3) atom is pushed toward the rocksalt layer with respect to the Mn atoms. The bond angle of the La compound is 177° , smaller than the ideal 180° , implying that the O(3) atoms are pulled inward to the perovskite layer. Therefore, the $\langle r \rangle_P$ in this case is smaller than that of the hole for this compound. With the decrease of $\langle r \rangle_{ave}$ the bond angle increases up to 184 - 185° for Ln = Gd and Eu. For the compounds of small Ln, the $\langle r \rangle_P$ is larger than that of the ideal Mn-O framework and has to deform the structure by pushing the O(3) atoms toward the rock salt layer. These changes are consistent with the slightly increasing $\langle r \rangle_P$ with decreasing $\langle r \rangle_{ave}$ in Table 2.

As a result of the shortening of the Mn-O(1) and Mn-(3) and the lengthening of the Mn-O(2) bond distances with the decrease of $\langle r \rangle_{ave}$, the MnO_6 octahedron becomes more distorted. In order to quantify the octahedral distortions, we have calculated two parameters in Table 2, namely, the Jahn-Teller parameter (D) and the distortion parameter (s) defined as in the following equations:

$$D = \langle Mn-O \rangle_{equatorial} / \langle Mn-O \rangle_{axial}$$

$$s = [1/6 \sum_i (\langle Mn-O \rangle - (Mn-O)_i)^2]^{1/2}$$

The Jahn-Teller parameter measures the degree of tetragonal distortion and the distortion parameter, the variance of the Mn-O bond distances, measures the degree of scatter of the bond distances. As can be seen in Table 2, the D param-

eters are smaller than unity for an undistorted octahedron and monotonically decrease on moving from La through Gd suggesting that the MnO_6 octahedron experiences more Jahn-Teller distortion with smaller Ln. The σ parameters also show that the La compound has the least distorted MnO_6 octahedron and the distortion increases on moving towards smaller Ln. However, for both of the two parameters, the largest change occurs in the La-Nd range and is nearly constant from Nd to Gd.

The physical properties of these compounds depend strongly on the nature of the Ln atoms as shown in Table 3.^{11,12} The La compound shows coincident ferromagnetic and insulator to metal transitions at 100 K. The saturated magnetic moment of this compound was 3.2 B.M from the susceptibility measurement and 3.0 B.M. from a powder neutron diffraction data refinement, showing that this compound follows the double exchange mechanism.¹⁷ However, the compounds of Pr-Sm show much reduced magnetic moments from the theoretical value. Moreover, the T_c 's of Pr and Nd compounds are much higher at 200-300 K than the T_{MN} 's. In fact, the resistivity data of the Nd compound shows that the metallic resistivity is still very large. It only shows a change of the temperature dependency of the resistivity, $d\rho/dT$, from negative to positive at about 70 K. The resistivity vs. temperature data of Pr is more or less the similar to that of the Nd compound. The powder neutron diffraction data of the Pr and Nd compounds did not show any sign of magnetic orderings demonstrating that the simple substitution of La by Pr and Nd result in drastic changes of the physical properties. The Sm compound is still different from those of the Pr and Nd compound. It has a reduced saturated magnetic moment. However, its T_c and T_{MN} coincide with each other. Moreover, the metallic resistivity of this compound is close to that of the La compound. The Gd and Eu compounds are paramagnetic insulators down to low temperatures.

The different physical properties depending on the nature of Ln is also reported on other $n = 2$ RP phases with different doping levels. Especially, the Ln = Nd compounds are studied extensively second to the Ln = La compounds. While the La compounds with different hole doping levels are more or less similar to one another in that they show coincident T_c 's and T_{MN} 's, the Nd compounds are reported to have either no or very weak signals of insulator to metal transitions.^{7,9-11} The difference was attributed to the different degree of the

Table 3. Summarized some physical properties of $Ln_{1.4}Sr_{1.6}Mn_2O_7$ (Ln = La, Pr, Nd, Sm, Eu, Gd). T_{MN} is metal-insulator transition temperature, MR ratio is $(\rho_0 - \rho_H)/\rho_H$, and M is maximum magnetic moment under 5,000G

Compounds	T_{MN} (K)	MR ratio (%)	T_c (K)	M (μ_B)
La-327	108	975(6T)	100	3.3
Pr-327	96	133(6T)	310	0.3
Nd-327	56	787(6T)	260	0.3
Sm-327	118	2362(3T)	110	0.36
Eu-327	no MIT	-	-	-
Gd-327	no MIT	-	-	-

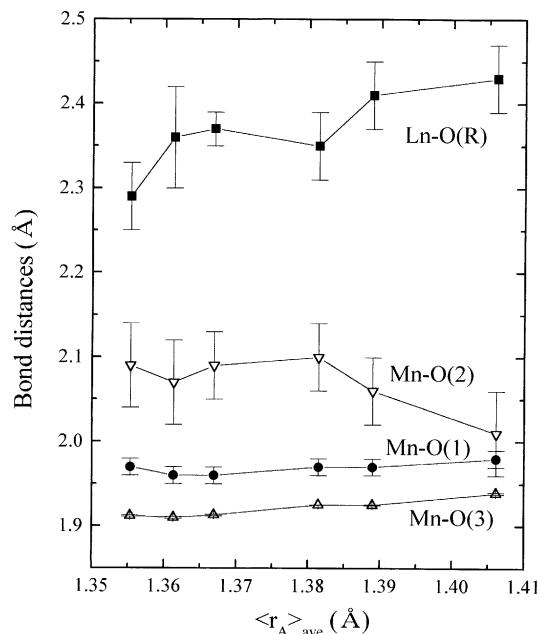


Figure 6. Variations of the bond distances of $\text{Ln}_{1.4}\text{Sr}_{1.6}\text{Mn}_2\text{O}_7$ ($\text{Ln} = \text{La}, \text{Pr}, \text{Nd}, \text{Sm}, \text{Eu}, \text{Gd}$) as a function of the average ionic radius of Ln and Sr from the Rietveld refinements on the powder X-ray diffraction patterns.

distortion of the MnO_6 octahedron, that is, the Nd compound gives more distortion and thus localized the otherwise itinerant e_g electron to suppress the metallic and ferromagnetic states. However, if the MnO_6 distortion is the only factor that influences the physical properties of these compounds, the D and σ parameters suggest that the compounds Nd-Gd should behave similarly, and the Pr compound should show an intermediate behavior between the La and Nd compounds which is not the case.

The structural variations with Ln in this series of layered compounds are manifold including the Ln/Sr occupancies, the lattice parameters, and the MnO_6 octahedral distortions. In addition, the magnetic properties of Ln atoms can influence the physical properties of these compounds. Above comparison of the crystal structure with the physical properties of our compounds indicates that the crystal structure alone cannot explain the variation of the physical properties. Therefore, we suggest that the magnetic properties of the Ln atoms play the dominating role in determining the physical properties of these compounds. In a recent paper on a series of $\text{LnSrMn}_{0.5}\text{Ni}_{0.5}\text{O}_4$ ($\text{Ln} = \text{La}, \text{Pr}, \text{Nd}, \text{Sm}, \text{Gd}$) compounds with the K_2NiF_4 type structure, we have shown that the magnetic interactions between neighboring layers strongly depend on the type of Ln atoms between the layers.¹⁸ Although the mechanism of this kind of inter-layer exchange interaction is not well established, the magnetic data of these layered compounds show strong relationship with the magnetic moments of Ln^{3+} ions. Because our present system resembles the K_2NiF_4 structure, we believe that the Ln-mediated inter-layer magnetic interaction is responsible for the destruction of the double exchange mechanism of the La compound.

In conclusion, we have systematically investigated the crystal structure of layered $\text{Ln}_{1.4}\text{Sr}_{1.6}\text{Mn}_2\text{O}_7$ ($\text{Ln} = \text{La}, \text{Pr}, \text{Nd}, \text{Sm}, \text{Eu}, \text{Gd}$) compounds whose physical properties show strong dependency on the nature of Ln. By comparing the variation of the Ln/Sr distribution between the P- and R-sites and the variations of the lattice parameters and bond distances, we have explained the relationship between these observations. Moreover, from these analyses we came to conclude that the crystal structure variation alone cannot explain the variations of the physical properties and that the magnetic properties of Ln in the interlayer must be responsible, instead.

Acknowledgment. Financial support for this research is from Korea Science and Engineering Foundation (KOSEF 971-0306-050-3).

References

- Moritomo, Y.; Asamitsu, A.; Kuwahara, H.; Tokura, Y. *Nature* **1996**, *380*, 141.
- Kimura, T.; Tomioka, Y.; Kuwahara, H.; Asamitsu, A.; Tamura, M.; Tokura, Y. *Science* **1996**, *274*, 1698.
- Kimura, T.; Asamitsu, A.; Tomioka, Y.; Tokura, Y. *Phys. Rev. Lett.* **1997**, *79*, 3720.
- Perring, T. G.; Aeppli, G.; Moritomo, Y.; Tokura, Y. *Phys. Rev. Lett.* **1997**, *78*, 3197.
- Argyriou, D. N.; Mitchell, J. F.; Goodenough, J. B.; Chmaissem, O.; Short, S.; Jorgensen, J. D. *Phys. Rev. Lett.* **1997**, *78*, 1568.
- Seshadri, R.; Martin, C.; Hervieu, M.; Raveau, B.; Rao, C. N. R. *Chem. Mater.* **1997**, *9*, 270.
- Battle, P. D.; Green, M. A.; Laskey, N. S.; Millburn, L. E.; Murphy, L.; Rosseinsky, M. J.; Sullivan, S. P.; Vente, J. F. *Phys. Rev. B* **1996**, *54*, 15967.
- Battle, P. D.; Green, M. A.; Laskey, N. S.; Kasmir, N.; Millburn, J. E.; Spring, L. E.; Sullivan, S. P.; Rosseinsky, M. J.; Vente, J. F. *J. Mater. Chem.* **1997**, *7*, 977.
- Battle, P. D.; Green, M. A.; Laskey, N. S.; Millburn, J. E.; Murphy, L.; Rosseinsky, M. J.; Sullivan, S. P.; Vente, J. F. *Chem. Mater.* **1997**, *9*, 552.
- Seshadri, R.; Martin, C.; Maignan, A.; Hervieu, M.; Raveau, B.; Rao, C. N. R. *J. Mater. Chem.* **1996**, *6*, 1585.
- Hur, N. H.; Kim, J.-T.; Yoo, K. H.; Park, Y. K.; Park, J. C.; Chi, E. O.; Kwon, Y.-U. *Phys. Rev. B* **1998**, *57*, 10740.
- Hur, N. H.; Chi, E. O.; Kwon, Y.-U.; Yu, J.; Kim, J.-T.; Park, Y. K.; Park, J. C. *Solid State Commun.* **1999**, *112*, 61.
- Izumi, F. *The Rietveld Method*; Young, R. A., Ed.: Oxford University Press: Oxford, 1993: Chap. 13.
- Kim, Y.-I.; Izumi, F. *J. Ceram. Soc. Jpn.* **1994**, *102*, 401.
- Shannon, R. D.; Prewitt, C. T. *Acta Crystallogr. B* **1969**, *25*, 925.
- Pauling, L. *The Nature of the Chemical Bond*, 3rd ed.; Cornell University: Ithaca, NY, 1960; p 239.
- Chi, E.-O.; Hong, K.-P.; Kwon, Y.-U.; Raju, N. P.; Greedan, J. E.; Lee, J.-S.; Hur, N. H. *Phys. Rev. B* **1999**, *60*, 12867.
- Hong, K.; Kwon, Y.-U.; Han, D.-K.; Lee, J.-S.; Kim, S.-H. *Chem. Mater.* **1999**, *11*, 1921.